I. Troch, F. Breitenecker, eds. ISBN 978-3-901608-35-3

Determination of Flux Directions by Thermodynamic Network Analysis: Computing Informative Metabolite Pools

F. Hadlich, W. Wiechert
Department of Simulation, University of Siegen, Germany
{frieder.hadlich, wolfgang.wiechert}@uni-siegen.de

Keywords: Metabolic Networks, Network Thermodynamics, Monte Carlo Method, Gibbs sampler, Flux Direction

Abstract

Network thermodynamics focuses on the energetic analysis of complex metabolic networks. The method connects free Gibbs energies (under standard conditions), metabolite concentrations and flux directions by thermodynamic laws. Here, a new application of network thermodynamics is presented, that determines those metabolite pools that have to be measured in order to determine as many flux directions as possible. For a medium scaled network informative pool sets are computed. It turns out that some reactions can already be directed with some few measurements and some reactions cannot be directed at all. Additionally, the results of measuring energetic currency metabolites is computed showing different effects.

Introduction

Presently, metabolomic and fluxomic data can be increasingly obtained. Many efforts are undertaken to create network models reflecting the complete metabolism. One popular way to receive more information about metabolism is including thermodynamic laws. Applications are given by consistency checking of mixed concentration/flux data, computing possible flux direction patterns [2, 6], or narrowing the feasible concentration space of unmeasured pools in biochemical networks [5].

Thermodynamic Concepts

To recall the effect of thermodynamics in metabolic reactions the example of a single reaction $v : S \rightarrow 2P$ is considered. Here, the (nominal) substrate S reacts to the (nominal) product P, but the opposite direction might also be possible. In general, the driving force (described by free Gibbs energy of reaction $\Delta_v G$) is determined from the free Gibbs energies of the reactants and the stoichiometry. Hence, the energy value of the reaction is defined by

$$\Delta_v G = 2 \cdot \Delta_P G - \Delta_S G. \tag{1}$$

For a negative driving force the flux v runs in nominal direction ($\mathsf{sign}(v) = 1$), whereas the opposite direction is defined by a positive $\Delta_v G$ value ($\mathsf{sign}(v) = -1$).

Under standard conditions (with one molar pool concentration) the pool formations have constant Gibbs energies. Under physiological conditions the free Gibbs energies of formation is computed by

$$\Delta_f G = \Delta_f G^0 + RT \cdot \ln x_f \tag{2}$$

including univsersal gas constant R, temperature T and concentration (in mole) x_f. Therefore the following thermodynamic law must hold:

$$0 > \mathsf{sign}(v) \cdot \left(2 \cdot \underbrace{\Delta_P G^0 + RT \cdot \ln x_P}_{\Delta_P G} - (\underbrace{\Delta_S G^0 + RT \cdot \ln x_S}_{\Delta_S G}) \right) \tag{3}$$

For this reaction datasets (x_S,x_P) are possible that refer to either nominal flux direction or to its opposition. In the case that $\Delta_v G^0$ is given with a positive value the flux arises in nominal direction ($\mathsf{sign}(v) = 1$) only if the concentration of S is much higher than the concentration of P.

Network Thermodynamics Analysis

The energetic analysis of complex metabolic networks with many reactions is done by so-called network thermodynamics [8]. Here, the idea of analysing a single reaction (as explained above) is extended to many reactions. For a given data set with information about all pools of the network, the method connects stoichiometric information (stoichiometric matrix $\mathbf{N}$ enhanced for system substrates and system products) in matrix $\mathbf{N}_{all}$, metabolite concentrations listed by vector $\mathbf{x}$, free Gibbs energies (under standard conditions) vector $\Delta_\mathbf{f}G^0$, and flux rate vector $\mathbf{v}$ by the vectorial thermodynamic law:

$$\mathbf{0} > \mathsf{diag}(\mathsf{sign}(\mathbf{v})) \cdot \mathbf{N}_{all}^T \cdot \left(\Delta_\mathbf{f}G^0 + RT \cdot \ln \mathbf{x}\right) \tag{4}$$

For most practical applications it makes sense to restrict the system to its steady states which implies that the fundamental mass-balance equations

$$\dot{\mathbf{x}} = \mathbf{N} \cdot \mathbf{v}(\mathbf{x}) = \mathbf{0}. \tag{5}$$

Furthermore, only models kept in steady state will be explored here.

Methods for network thermodynamic analysis are performed using two types of data uncertainty. There are insecure information about free Gibbs energies (under standard conditions) and about pool concentrations. These can be addressed using tolerance intervals:

$$\begin{array}{ccccc} \Delta_\mathbf{f}G^0_{min} & \leq & \Delta_\mathbf{f}G^0 & \leq & \Delta_\mathbf{f}G^0_{max} \\ \mathbf{x}_{min} & \leq & \mathbf{x} & \leq & \mathbf{x}_{max} \end{array} \tag{6}$$

Equations 4-6 now allow to reduce the set of feasible flux direction patterns $\mathbf{FDP}^{feas}$:

$$\mathbf{FDP} = \left\{ \mathsf{sign}(v) \;\middle|\; \begin{array}{ccccc} \mathbf{0} > \mathsf{diag}(\mathsf{sign}(\mathbf{v})) \cdot \mathbf{N}_{all}^T \cdot \left(\Delta_\mathbf{f}G^0 + RT \cdot \ln \mathbf{x}\right) & & & & \\ \mathbf{N} & \cdot & \mathbf{v}(\mathbf{x}) & = & \mathbf{0} \\ \Delta_\mathbf{f}G^0_{min} & \leq & \Delta_\mathbf{f}G^0 & \leq & \Delta_\mathbf{f}G^0_{max} \\ \mathbf{x}_{min} & \leq & \mathbf{x} & \leq & \mathbf{x}_{max} \\ & & \mathsf{sign}(v) & \in & \mathbf{FDP}^{\mathrm{feas}} \end{array} \right\}. \tag{7}$$

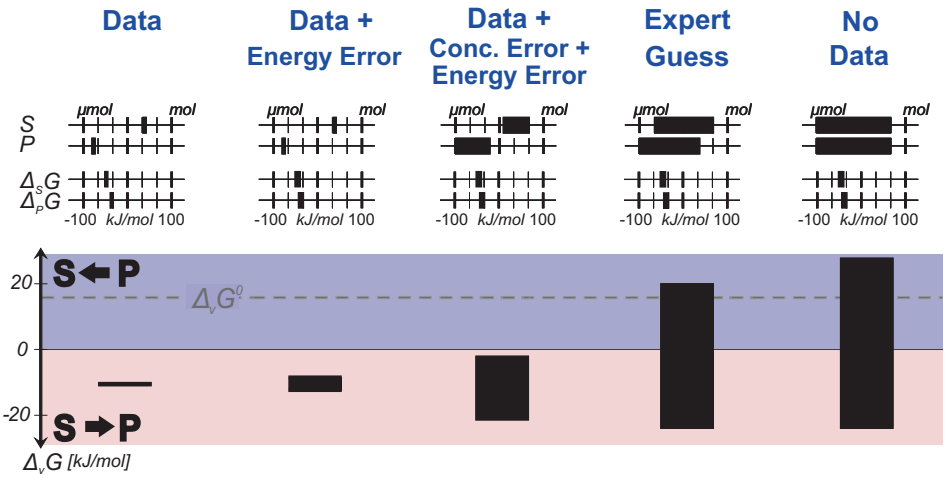

Figure 1: Effect of data uncertainty on flux direction prediction by computing Gibbs energy of reaction: the energy is a value for exact data (left result) but forms an interval for data uncertainty (other results).

The effect of data uncertainty concerning prediction of flux direction is presented in Figure 1 for these different cases:

- In the ideal case exact data is given for all pools and the exact Gibbs value are known for the reaction.

$$\Delta_{\mathbf{f}} G^0_{min} = \Delta_{\mathbf{f}} G^0_{max}, \qquad \mathbf{x}_{min} = \mathbf{x}_{max}$$

  In this case **FDP** reduces to at most one element.

- Unfortunately, the free Gibbs energy value cannot be directly measured and different assumptions have to be made [1, 7]. Hence, the energy value is only given in (mainly small) intervals:

$$\Delta_{\mathbf{f}} G^0_{min} \approx \Delta_{\mathbf{f}} G^0_{max}, \qquad \mathbf{x}_{min} = \mathbf{x}_{max}.$$

  This might already allow for multiple **FDP** elements.

- Commonly, measurements are noisy which is caused by complicated measurement protocols. Therefore, a confidence interval has to be added to the exact data:

$$\Delta_{\mathbf{f}} G^0_{min} \approx \Delta_{\mathbf{f}} G^0_{max}, \qquad \mathbf{x}_{min} \approx \mathbf{x}_{max}.$$

  The number of elements in **FDP** typically increases.

- In most cases, concentration cannot be measured and Gibbs values are noisy. Thus, only expertise know-how (i.e. from similar experiments) can help limiting the concentration range:

$$\Delta_{\mathbf{f}} G^0_{min} \approx \Delta_{\mathbf{f}} G^0_{max}, \qquad \mathbf{x}_{min} < \mathbf{x}_{max}.$$

  Here, **FDP** usually contains most $\mathbf{FDP}^{feas}$ elements.

- The worst case of prediction uncertainty is given if there is no limiting pool information available and, consequently, all data combinations last being acceptable:

$$\Delta_{\mathbf{f}} G^0_{min} \approx \Delta_{\mathbf{f}} G^0_{max}, \qquad \mathbf{x}_{min} \ll \mathbf{x}_{max}.$$

  In this case **FDP** enlarges to all $\mathbf{FDP}^{feas}$ elements.

For further investigations the mostly weak effect of energy uncertainty is neglected and constant standard Gibbs values are assumed. They are calculated using Alberty's method [1].

In the concert of network thermodynamics all reactions effect each other by limiting the tolerated data intervals. Therefore, new constraints appear in the concentration space which cannot be easily understood in the high-dimensional space. One way of approximately exploring the thermodynamically feasible concentration space is done by using the tool annet [10], which offers narrowed concentration limits (based on constant standard energy values).

Concept of the new method

Here, a new application of network thermodynamics is presented that determines those metabolite pools that have to be measured in order to determine as many flux directions as possible. Therefore, the following questions can be addressed:

- Which information is contained in one or more measurable pools on the direction of all $\mathbf{FDP}^{feas}$ elements?
- Which direction information is given by a specific set of measurable pools?
- Which metabolite pools in a given network need to be measured for determining a specific flux direction?
- Are there reactions whose direction cannot be determined at all?
- How important is the measurement of energetic currency metabolites ATP, ADP, NAD, NADH etc.?

Before answering these questions an illustration of principle will be given.

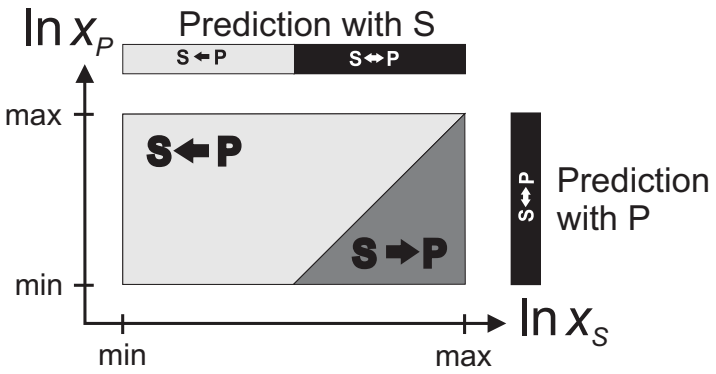

Figure 2: Feasible concentration space used in the simple reaction with its bisections given by thermodynamic flux direction analysis

Illustration of Principle

The prediction of the flux direction with measurements can be explained using the introduced simple reaction. Figure 2 shows a proper concentration space that is divided in two subspaces describing unique flux directions.

- In case that both pools S and P are measured the flux direction is always uniquely determinable if no data uncertainty appears.
- If the set of measurable pools contains only pool P, no predictive can be made. For every value of P both directions are feasible in concentration space.
- Suspecting S as measured enables the prognose of a unique flux direction for a low concentration. Here, for a low pool size the flux direction is contra-nominal ($\mathsf{sign}(v) = -1$).
- Given the case that neither S nor P are contained in the data vector, no direction prediction can be made. However, in the context of a larger network, this might well be the case.

Optimal solution

The answers to the addressed questions will be given in probabilistic terms, i.e. a probability is assigned to each flux pattern given the measured data. This is done as follows:

1. A log-uniform distribution is assumed in the thermodynamically feasible concentration space of all metabolites in the network constrained by Equation 4 with $\mathbf{N}_{dir}$ and $\mathbf{v}_{dir}$ ($\mathbf{N}_{all}$, $\mathbf{v}$ without undirected fluxes) instead of $\mathbf{N}_{all}$ and $\mathbf{v}$ permitting all $\mathbf{FDP}^{feas}$ elements. The logarithmized scaling of space dimensions is needed to form realistic data distributions.
2. The high-dimensional distribution is projected to the subspace with the specific set of measurable pools. Afterwards the uniformity of the distribution gets lost and interesting arrangements occur (histogram results for a single fixed pool are given in [9]). Furthermore, the distributions in subspace are used to imitate realistic measured data distributions.
3. For a specific reversible reaction the low-dimensional distribution is checked how far the possible measured values uniquely determine its net flux direction. Because each network reaction that is defined to be unidirectional constrains the feasible concentration space the specific reaction v is now set to be directed, too. Consequently $\mathbf{N}_{dir}$ and $\mathbf{v}$ are enlarged for reaction v. For the forward and the backward directed flux two different sets of flux direction patterns $\mathbf{FDP}^{\mathsf{sign}(v)=-1}$ and $\mathbf{FDP}^{\mathsf{sign}(v)=1}$ with $\mathbf{FDP}^{\mathsf{sign}(v)=|1|} \in \mathbf{FDP}^{feas}$ are generated describing two separate solution spaces. Furthermore, these solution spaces are assigned to the low-dimensional distribution.
4. The probability of unique flux direction determination from the subspace distribution is taken as a measure of information.

Monte Carlo solution

The practical realization of this analytic concept requires an approximation with a Monte Carlo approach. In this work the prediction of net flux directions for a specific set of measurable pools is performed similar to the analytic operations. The steps are schematically shown in Figure 3.

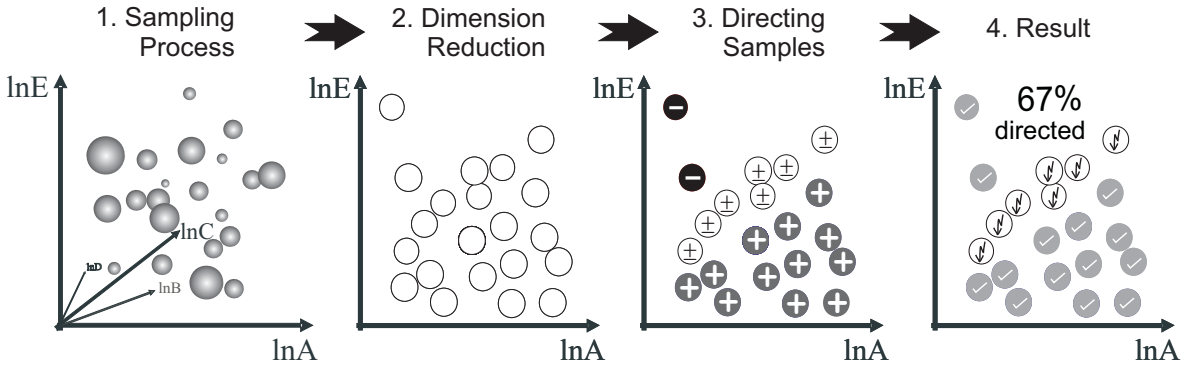

Figure 3: General steps of the flux direction determination for the measurable pools A and E.

Necessary operations to perform the numerical solution are:

1. Samples are generated in the thermodynamically feasible concentration space (within $\mathbf{x}_{min} \leq \mathbf{x} \leq \mathbf{x}_{max}$) of all metabolites in the network. Therefore the Markov Chain Monte Carlo based Gibbs sampler [3] is used to uniformly distribute the samples in the logarithmized concentration space.

2. Each high-dimensional sample vector is reduced to a low-dimensional one by keeping the dimensions (numbers given in vector $\mathbf{p}$) of the specific set of measurable pools. Each minimized sample vector $\tilde{\mathbf{x}}^{\mathbf{p}} = \tilde{x}^{p_1} \cdots \tilde{x}^{p_n}$ imitates real measurements.

3. Every sample vector $\tilde{\mathbf{x}}^{\mathbf{p}}$ is checked for its affiliation to one or both flux directions of reaction v by solving the optimization problems

$$\Delta_{v_{fw}} G(\tilde{\mathbf{x}}^{\mathbf{p}}) = \min_{\substack{\mathbf{x}_{min} \leq \mathbf{x} \leq \mathbf{x}_{max} \\ \mathbf{N}\cdot\mathbf{v}=0 \\ \mathbf{x}^{\mathbf{p}}_{min} \leq \mathbf{x} \leq \mathbf{x}^{\mathbf{p}}_{max} \\ x^{p_1}=\tilde{x}^{p_1},\cdots,x^{p_n}=\tilde{x}^{p_n} \\ \mathsf{sign}(v)=1}} \mathsf{diag}(\mathsf{sign}(\mathbf{v}_{dir})) \cdot \mathbf{N}_{dir}^T \cdot \left(\Delta_{\mathbf{f}} G^0 + RT \cdot \ln \mathbf{x}\right) \tag{8}$$

and

$$\Delta_{v_{bw}} G(\tilde{\mathbf{x}}^{\mathbf{p}}) = \max_{\substack{\mathbf{x}_{min} \leq \mathbf{x} \leq \mathbf{x}_{max} \\ \mathbf{N}\cdot\mathbf{v}=0 \\ \mathbf{x}^{\mathbf{p}}_{min} \leq \mathbf{x} \leq \mathbf{x}^{\mathbf{p}}_{max} \\ x^{p_1}=\tilde{x}^{p_1},\cdots,x^{p_n}=\tilde{x}^{p_n} \\ \mathsf{sign}(v)=-1}} \mathsf{diag}(\mathsf{sign}(\mathbf{v}_{dir})) \cdot \mathbf{N}_{dir}^T \cdot \left(\Delta_{\mathbf{f}} G^0 + RT \cdot \ln \mathbf{x}\right). \tag{9}$$

Here, $\mathbf{x}$ contains concrete values for measurable pools and concentration intervals for the unknown pools. The affiliation of this sample vector to one or both flux directions is computed by

$$\mathit{aff}_v(\tilde{\mathbf{x}}^{\mathbf{p}}) = \left(\Delta_{v_{fw}} G(\tilde{\mathbf{x}}^{\mathbf{p}}) < 0\right) \otimes \left(\Delta_{v_{bw}} G(\tilde{\mathbf{x}}^{\mathbf{p}}) > 0\right) \tag{10}$$

and returns $\mathit{aff}_v(\tilde{\mathbf{x}}^{\mathbf{p}}) = \mathbf{true}$ if exactly one flux direction is possible, otherwise $\mathit{aff}_v(\tilde{\mathbf{x}}^{\mathbf{p}}) = \mathbf{false}$.

4. As final step, the probability $d_{v,\mathbf{p}}$ of unique flux direction of reaction v is determined by computing the relative density of all samples $(\tilde{\mathbf{x}}^{\mathbf{p}}_1, \cdots, \tilde{\mathbf{x}}^{\mathbf{p}}_m)$ affiliation:

$$d_{v,\mathbf{p}} = \frac{1}{m} \sum_{i=1}^{m} \mathit{aff}_v(\tilde{\mathbf{x}}^{\mathbf{p}}_i). \tag{11}$$

Example Application

For a medium-scaled metabolic network the application of flux direction prediction is done.

Network

A typical metabolic network that has been analyzed describes the central carbon metabolism of *C.glutamicum*. More details about this microorganism are published in [4]. As shown in Figure 4 this network contains 42 pools that are inter-connected by 36 reactions. 18 of these reactions are assumed to be unidirectional apriori. The 23 grey-colored pools in Figure 4 are measurable. Initially, for each pool a wide range is given with lower ($10\mu mol/gdw$) and upper concentration limits ($0.1mol/gdw$). Only the concentration of water is assumed to be constant.

In steady state some flux directions are directly coupled to each other by stoichiometry. Concrete correlations (shown in Figure 4) occur in the tested network like the one between the reversible reactions *pglumu* and *eno*. For this reason, the number of reaction directions that have to be predicted significantly decreases in this network. More precisely, directions of 13 reactions or correlated reaction bundles have to be determined.

The flux direction prediction is accomplished as explained in concept chapter. Here, one thousand samples are tested for having a unique flux direction for different subsets of all measurable pools by solving Equation 8. Performing the analysis for every possible subset of the metabolite pools is a combinatorial problem of high complexity. Limiting the patterns to at most three pools already results in almost two thousand different patterns in the tested case and, of course, each pool pattern is checked with 13 single reactions or correlated reaction bundles. Consequently, the analysis is performed only for one, two and three measurable pools for the presented network of *C.glutamicum*.

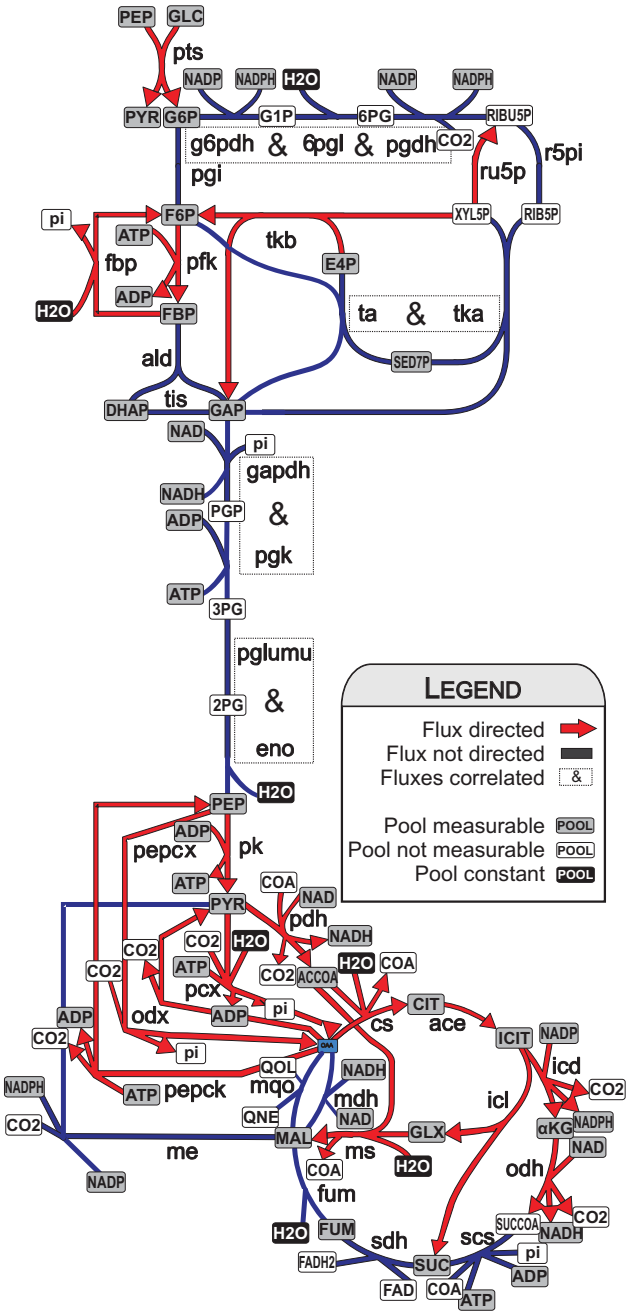

Figure 4: Network structure of the central metabolism of *C. glutamicum*

Pool pattern	Reaction	Result (%)
PEP	eno, pglumu	91.5
GAP	tis	81.6
MAL	fum	68.6
FUM	fum	59.3
DHAP	tis	33.5
MAL NAD	mdh	61.8
MAL NADH	mdh	61.7
G6P NADPH	g6pdh pgdh 6pgl	57.3
G6P NADP	g6pdh pgdh 6pgl	57.2
DHAP E4P	tis	51.9
G6P NADP NADPH	g6pdh pgdh 6pgl	97.2
MAL NAD NADH	mdh	88.7
DHAP E4P F6P	tis	65.5
DHAP E4P FBP	ald	42.5
E4P G6P GAP	pgi	42.2

Pool pattern	Result (%)
PEP	7.0
MAL	6.9
GAP	6.3
FUM	4.6
DHAP	2.6
MAL PEP	14.0
GAP PEP	13.3
GAP MAL	13.2
FUM PEP	11.6
FUM GAP	10.8
GAP MAL PEP	20.2
FUM GAP PEP	17.9
MAL NAD PEP	17.1
MAL NADH PEP	17.1
DHAP MAL PEP	16.5

Table 1: Nontrivial local results (left table) and global results (right table) for measurable pool patterns of size one, two and three

Local results

The output ends up with trivial and nontrivial results which belong to a single (or local) reaction. Trivial results can directly be derived if all substrate and all product pools of the tested reversible reaction are measured. An example is given by reaction *tis* and the pools *DHAP* and *GAP*. Clearly, if both pools (that are all pools reacting in *tis*) are measured the direction of *tis* is determined. In opposition to trivial cases, nontrivial cases are not obvious from the measured pool pattern. Here, one or more pools are missing to build a trivial case. A nontrivial example is given by reaction *eno*. Even if *PEP* can be measured *eno*'s direction cannot be completely derived without knowing *2PG*, which is not measurable at all. A list of nontrivial results computed by Equation 11 is given on the left side of Table 1.

If only measurements of a single pool are available for the tested network it is, nevertheless, possible to predict some flux directions with a high probability. For the case of pool *PEP* the correlated fluxes *eno* and *pglumu* can be directed for almost every sample (91%). Clearly, the influence of two or more pools is higher or at least equal to the added influence of the single pools. Consequently, all measurable pools that are combined to *PEP* will return the same or even a better result for *eno* and *pglumu*. Pool patterns with the same results like single pools are neglected in the listing of Table 1.

If a data set contains more than one measurement reversible reactions like *mdh*,*ald* and *pgi* become predictable in their flux direction. Valuable information is delivered from the pool *G6P* and the energetic currency metabolites *NADP* and *NADPH*: Their measurement can be used to determine the flux directions of three correlated reactions (*g6pdh*,*pgdh* and *6pgl*) for almost every data set (97%).

Interestingly, for some cases the pools aren't even attached to the affected reaction. This happens in the special case of reaction *tis* when the measurement of the non-related pools *E4P* and *F6P* together with the attached pool *DHAP* makes sense (65%). Without measuring the detached pools this reaction direction is much less determined (33%).

For some reactions the investigations made are not fruitful: The tested reversible reaction *r5pi* effects no checked sample of any tested pool pattern. Reasons might be that none of the attached pools is measurable, and the reaction plays no central role in the described metabolism. Even two reactions (*scs* and *sdh*) of the TCA cycle show almost no effect although many of their affected pools can be measured.

Global results

Additionally to the (local) effects of a pool pattern concerning single reactions (and correlated reactions) its (global) predictive power is interesting for all reversible reactions. The realized measure of the global influence $g_{\mathbf{p}}$ of pool pattern $\mathbf{p}$ is computed by the mean

$$g_{\mathbf{p}} = \frac{1}{n} \sum_{i=1}^{n} d_{v_i,\mathbf{p}} \tag{12}$$

including the local influence $d_{v_i,\mathbf{p}}$ of each reaction v_i. On the right side of Table 1 the best results concerning the global effect are listed for pool size one, two and three.

The best globally predicting pools are *GAP*, *MAL* and *PEP*. One of these pools measured stand-alone can determine approximately one of all unknown flux directions. Because the three pools affect different reactions their joining is very informative (20% of all reversible fluxes). In contrast, patterns that are made up by reaction-sharing pools are not that valuable. Fortunately, some pool patterns even present better global influences than expected: The pattern given by *NAD*, *MAL* and *PEP* confirms 17% global influence, expectable are just 14% as sum of the single pools influences.

Because cofactors are involved in many reversible reactions their measurement is expected to be very important. This assumption is confirmed for many but not all cofactors in the given network of *C.glutamicum*'s central metabolism. In combination with other pools the measurement of *NAD*, *NADH*, *NADP* or *NADPH* is profitable for direction predictions. In contrast, the measurement of both energetic counterparts (i.e *NAD* and *NADH*) is unproductive.

Interestingly, there are hardly global effects obtained for the energetic currency metabolites *ADP* and *ATP*. A reason might be that these cofactors are involved in only two undirected reactions of the tested metabolism. If a reaction link between these two and other cofactors (i.e. oxidative phosphorylation) is included, they can play a superordinate role in global view.

Conclusion and Outlook

The prediction of flux directions is realizable with the explained concept based on thermodynamical data. Therefore, exact concentration measurements are generated *in-silico* in preset concentration intervals. Thus, data uncertainty is included for measurements, but uncertainty of standard Gibbs values is neglected. For a small metabolic network concrete answers are given to all central questions. Summarizing the results yields these conclusions:

- Given pool measurements the prediction of flux directions can be computed with Monte Carlo sampling. Some specific flux directions cannot be predicted by measurements at all, others are almost completely determined with just one measurement.
- Pools that are involved in many reactions have more influence on undirected fluxes than pools that participate in few reactions.
- Clearly, the more pools are measured the more fluxes become predictable. But, thereby the informative increase becomes smaller.

The used algorithm to generate the presented results is a fundamental prototype, and further developments will follow. With an improved concept the handling of several thousand samples in large scaled networks is intended. Furthermore, the exploration of pool patterns with more than three measurements and the behavior of grouped undirected reactions are of interest.

Acknowledgement

This work was funded by the Evonic Industries and the German Ministry of Education and Research within the SysMAP project (BMBF 0313704).

References

[1] Alberty, R. A. Calculation of thermodynamic properties of species of biochemical reactants using the inverse legendre transform. *The journal of physical chemistry. B 109*, 18 (2005), 9132–9139.

[2] Beard, D. A., Liang, S.-d., and Qian, H. Energy balance analysis of complex metabolic networks. *Biophysical Journal 83* (2002), 79–86.

[3] Casella, G., and George, E. I. Explaining the gibbs sampler. *American Statistical Association 46*, 3 (1992), 167–174.

[4] Eggeling, L., and Bott, M. *Handbook of Corynebacterium Glutamicum*. CRC Press, 2005.

[5] Henry, C. S., Broadbelt, L. J., and Hatzimanikatis, V. Thermodynamics-based metabolic flux analysis. *Metabolic Engineering 92* (2007), 1792–1805.

[6] Henry, C. S., Jankowski, M. D., Broadbelt, L. J., and Hatzimanikatis, V. Genome-scale thermodynamic analysis of escherichia coli metabolism. *Biophysical Journal 90* (2006), 1453–1461.

[7] Jankowski, M. D., Henry, C. S., Broadbelt, L. J., and Hatzimanikatis, V. Group contribution method for thermodynamic analysis of complex metabolic networks. *Biophysical Journal 95* (2008), 1487–1499.

[8] Kümmel, A., Panke, S., and Heinemann, M. Systematic assignment of thermodynamic constraints in metabolic network models. *BMC Bioinformatics 7*, 512 (2006).

[9] Schellenberger, J., Tsai, E. A., and Palsson, B. O. Exploring the concentration space of genome scale metabolic networks. In *International Conference on Systems Biology* (Long Beach, California, 2007), vol. 8.

[10] Zamboni, N., Kümmel, A., and Heinemann, M. annet: a tool for network-embedded thermodynamic analysis of quantitative metabolome data. *BMC Bioinformatics 9*, 199 (2008).